A basic model of calcium homeostasis in non-excitable cells

Christina H. Selstø, Peter Ruoff*

Department of Chemistry, Bioscience, and Environmental Engineering, University of Stavanger, Stavanger, Norway

Supporting Information S3 Text

Dicalcic model

The scheme of the model to describe the influence of cytosolic Ca concentration on the transport of Ca ions out of the endoplasmatic reticulum (ER) into the cytoplasm by IP3R is shown in Fig. S1.

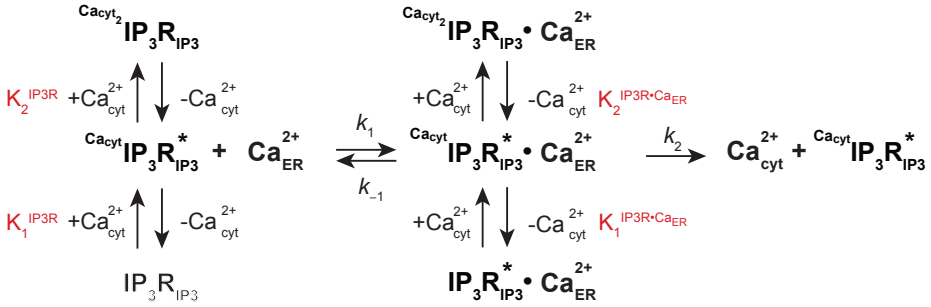

Figure S1. Dual Calcium binding model. The model consists of two cytosolic Ca binding sites, one that activates the IP3R transporter when Ca ion concentration is low, whereas at higher cytosolic Ca concentrations binding to the second site inhibits IP_3R. The dissociation constants are outlined in red.

The dynamic structure of the model is analogous to a diprotic model describing the influence of pH on an enzyme's catalytic activity [1]. The transporter IP_3R needs to have bound IP_3 to function and we assume that we have a complex between IP_3R and IP_3 present described as IP_3R_{IP3} (Fig. S1). The transporter kinetics of IP_3R are written as Michaelis-Menten kinetics where Ca in the ER binds to the "catalytic/transporter" site of the transporter and moves it into the cytosol with associated rate constants k_1, k_{-1}, and k_2. In addition to the transport site of IP_3R the model contains two Ca binding site, one activating the other inactivating the transporter. In the model the transporting form of IP_3R has one *cytosolic* Ca ion bound at the activating site and is indicated by ${}^{\mathrm{Ca_{cyt}}}\mathrm{IP_3R_{IP3}}^*$ (Fig. S1).

The dissociation constants K_1^{IP3R} and K_2^{IP3R}

$$K_1^{IP3R} = \frac{(\mathrm{Ca}^{2+}_{\mathrm{cyt}})(\mathrm{IP_3R_{IP3}})}{({}^{\mathrm{Ca_{cyt}}}\mathrm{IP_3R_{IP3}}^*)} \tag{S1}$$

$$K_2^{IP3R} = \frac{(\mathrm{Ca}^{2+}_{\mathrm{cyt}})({}^{\mathrm{Ca_{cyt}}}\mathrm{IP_3R_{IP3}}^*)}{({}^{\mathrm{Ca_{cyt_2}}}\mathrm{IP_3R_{IP3}})} \tag{S2}$$

describe the activation of IP_3R_{IP3} by cytosolic Ca binding leading to the active form ${}^{Ca_{cyt}}IP_3R_{IP3}{}^*$, and its inactivation by the second binding of cytosolic Ca, leading to ${}^{Ca_{cyt_2}}IP_3R_{IP3}$, respectively.

The active form ${}^{Ca_{cyt}}IP_3R_{IP3}{}^*$ binds Ca from the ER (Ca^{2+}_{ER}), giving ${}^{Ca_{cyt}}IP_3R_{IP3}{}^*\bullet Ca^{2+}_{ER}$, which transports Ca^{2+}_{ER} into the cytosol. The rate of transport, v, is described by

$$v = k_2({}^{Ca_{cyt}}IP_3R_{IP3}{}^*\bullet Ca^{2+}_{ER}) \tag{S3}$$

${}^{Ca_{cyt}}IP_3R_{IP3}{}^*\bullet Ca^{2+}_{ER}$ can either release the allosterically bound Ca back into the cytosol giving transporter-inactive form $IP_3R_{IP3}\bullet Ca^{2+}_{ER}$ or bind another cytosolic Ca and lead to the other inactive form ${}^{Ca_{cyt_2}}IP_3R_{IP3}\bullet Ca^{2+}_{ER}$. The assumed equilibria considered to occur in relation to these two processes are described by the two dissociation constants $K_1^{IP3R\cdot Ca_{ER}}$ and $K_2^{IP3R\cdot Ca_{ER}}$, respectively

$$K_1^{IP3R\cdot Ca_{ER}} = \frac{(Ca^{2+}_{cyt})(IP_3R_{IP3}\bullet Ca^{2+}_{ER})}{({}^{Ca_{cyt}}IP_3R_{IP3}{}^*\bullet Ca^{2+}_{ER})} \tag{S4}$$

$$K_2^{IP3R\cdot Ca_{ER}} = \frac{(Ca^{2+}_{cyt})({}^{Ca_{cyt}}IP_3R_{IP3}{}^*\bullet Ca^{2+}_{ER})}{({}^{Ca_{cyt_2}}IP_3R_{IP3}\bullet Ca^{2+}_{ER})} \tag{S5}$$

In comparison with experiments [2] v is proportional to observed IP_3R channel open probabilities at different IP_3 concentrations as a function of Ca concentration (see Fig. 1 in Ref. [2]).

In deriving an expression for v showing its dependence on cytosolic Ca as well as the activator IP_3 we assume that the total amount of transporter IP_3R, IP_3R_0, is constant with the mass balance

$$\begin{aligned} IP_3R_0 = {} & IP_3R_{IP3} + {}^{Ca_{cyt}}IP_3R_{IP3}{}^* + {}^{Ca_{cyt_2}}IP_3R_{IP3} \\ & + IP_3R_{IP3}\bullet Ca^{2+}_{ER} + {}^{Ca_{cyt}}IP_3R_{IP3}{}^*\bullet Ca^{2+}_{ER} + {}^{Ca_{cyt_2}}IP_3R_{IP3}\bullet Ca^{2+}_{ER} \end{aligned} \tag{S6}$$

In addition to the above equations, we also assume that the reactive form of the transporter, ${}^{Ca_{cyt}}IP_3R_{IP3}{}^*\bullet Ca^{2+}_{ER}$, is in a steady state, i.e.,

$$\frac{d({}^{Ca_{cyt}}IP_3R_{IP3}{}^*\bullet Ca^{2+}_{ER})}{dt} = 0 \tag{S7}$$

In analogy with Michaelis-Menten kinetics Eq. S7 leads to a dynamical equilibrium constant corresponding to the Michaelis constant K_M which relates Ca^{2+}_{ER} and ${}^{Ca_{cyt}}IP_3R_{IP3}{}^*$ with ${}^{Ca_{cyt}}IP_3R_{IP3}{}^*\bullet Ca^{2+}_{ER}$, i.e.,

$$K_M = \frac{(Ca^{2+}_{ER})({}^{Ca_{cyt}}IP_3R_{IP3}{}^*)}{({}^{Ca_{cyt}}IP_3R_{IP3}{}^*\bullet Ca^{2+}_{ER})} = \frac{k_{-1}+k_2}{k_1} \tag{S8}$$

By using Eqs. S1 and S2 IP_3R_{IP3} and ${}^{Ca_{cyt_2}}IP_3R_{IP3}$ can be expressed in terms of ${}^{Ca_{cyt}}IP_3R_{IP3}{}^*$. Likewise, by using Eqs. S4 and S5, $IP_3R_{IP3}\bullet Ca^{2+}_{ER}$ and ${}^{Ca_{cyt_2}}IP_3R_{IP3}\bullet Ca^{2+}_{ER}$ and be expressed in terms of ${}^{Ca_{cyt}}IP_3R_{IP3}{}^*\bullet Ca^{2+}_{ER}$. Thus, the mass balance Eq. S6 can be rewritten as

$$IP_3R_0 = f_{IP3R}({}^{Ca_{cyt}}IP_3R_{IP3}{}^*) + f_{IP3R\cdot Ca}({}^{Ca_{cyt}}IP_3R_{IP3}{}^*\bullet Ca^{2+}_{ER}) \tag{S9}$$

where

$$f_{IP3R} = 1 + \frac{K_2^{IP3R}}{Ca^{2+}_{cyt}} + \frac{Ca^{2+}_{cyt}}{K_1^{IP3R}} \tag{S10}$$

and

$$f_{IP3R\cdot Ca_{ER}} = 1 + \frac{K_2^{IP3R\cdot Ca_{ER}}}{\mathrm{Ca}_{\mathrm{cyt}}^{2+}} + \frac{\mathrm{Ca}_{\mathrm{cyt}}^{2+}}{K_1^{IP3R\cdot Ca_{ER}}} \tag{S11}$$

By using Eq. S8 ${}^{\mathrm{Ca_{cyt}}}\mathrm{IP_3R_{IP3}}^*$ can be expressed in terms of ${}^{\mathrm{Ca_{cyt}}}\mathrm{IP_3R_{IP3}}^* \bullet \mathrm{Ca}_{\mathrm{ER}}^{2+}$

$${}^{\mathrm{Ca_{cyt}}}\mathrm{IP_3R_{IP3}}^* = \frac{K_M}{\mathrm{Ca}_{\mathrm{ER}}^{2+}} \left({}^{\mathrm{Ca_{cyt}}}\mathrm{IP_3R_{IP3}}^* \bullet \mathrm{Ca}_{\mathrm{ER}}^{2+}\right) \tag{S12}$$

which, when inserted into Eq. S9 gives

$$\mathrm{IP_3R_0} = \left(f_{IP3R} \cdot \frac{K_M}{\mathrm{Ca}_{\mathrm{ER}}^{2+}} + f_{IP3R\cdot Ca_{ER}} \right) ({}^{\mathrm{Ca_{cyt}}}\mathrm{IP_3R_{IP3}}^* \bullet \mathrm{Ca}_{\mathrm{ER}}^{2+}) \tag{S13}$$

Solving for ${}^{\mathrm{Ca_{cyt}}}\mathrm{IP_3R_{IP3}}^* \cdot \mathrm{Ca}_{\mathrm{ER}}^{2+}$ from Eq. S13 and inserting it into Eq. S3 gives an expression of how v will depend on $\mathrm{Ca}_{\mathrm{ER}}^{2+}$ and $\mathrm{Ca}_{\mathrm{cyt}}^{2+}$

$$v = \frac{V_{max} \cdot (\mathrm{Ca}_{\mathrm{ER}}^{2+})}{f_{IP3R} \cdot K_M + f_{IP3R\cdot Ca_{ER}} \cdot (\mathrm{Ca}_{\mathrm{ER}}^{2+})} \tag{S14}$$

where V_{max}=k_2·($\mathrm{IP_3R_0}$).

Allosteric Inhibition of $\mathrm{IP_3R}$ by Calcium

Kaftan et al. [2] studied the $\mathrm{IP_3R}$ transporter activities at different Ca and $\mathrm{IP_3}$ concentrations by using canine cerebellar endoplasmatic reticulum vesicles which were fused with planar lipid bilayers. To make their experimental results comparable with the dual Ca model we equate their observed channel open probability with v described by Eq. S14. To simplify our model we make the assumption that $K_1^{IP3R\cdot Ca_{ER}} = K_1^{IP3R}$ $= K_2^{IP3R\cdot Ca_{ER}} = K_2^{IP3R}$. In the model the effect of Ca on $\mathrm{IP_3R}$ is a two-fold, Ca residing at the ER side of the transporter is moved into the cytosol, while cytosolic Ca activate or inhibit $\mathrm{IP_3R}$ from the cytosolic site. To compare v with the reported channel open probabilities in % V_{max} values are scaled to % channel open probability. In addition, we have used fixed values for K_M=0.01 μM and 1 μM for $\mathrm{Ca}_{\mathrm{ER}}^{2+}$.

Fig. S2 shows the results of fitting v (Eq. S14) to the experimental channel open probabilities. The dicalcic model shows good fits for the activation of $\mathrm{IP_3R}$ by cytosolic Ca for increasing $\mathrm{IP_3}$ concentrations with relative little changes in the dissociation constants. V_{max} increases with increasing $\mathrm{IP_3}$ concentration showing a good fit to a saturating function $f(x) = a{\cdot}x/(b+x)$ (Fig. S3). However, except for the 180 μM $\mathrm{IP_3}$ data the model shows a less rapid decrease in the transporter activity with increasing $\mathrm{Ca}_{\mathrm{cyt}}^{2+}$ (decreasing pCa) than observed experimentally (Fig. S2).

In view of numerous cytosolic Ca binding sites of the transporter (Fig. 10) we tested whether (at least) two allosteric inhibitory binding sites for cytosolic Ca may give a decreased half-width of the v-pCa bell-shaped curve by considering the following binding reactions

$${}^{\mathrm{Ca_{cyt}}}\mathrm{IP_3R_{IP3}}^* + 2\,\mathrm{Ca}_{\mathrm{cyt}}^{2+} \rightleftarrows {}^{\mathrm{Ca_{cyt_3}}}\,\mathrm{IP_3R_{IP3}} \tag{S15}$$

with

$$K_2^{IP3R} = \frac{(\mathrm{Ca}_{\mathrm{cyt}}^{2+})^2({}^{\mathrm{Ca_{cyt}}}\mathrm{IP_3R_{IP3}}^*)}{({}^{\mathrm{Ca_{cyt_3}}}\mathrm{IP_3R_{IP3}})} \tag{S16}$$

and

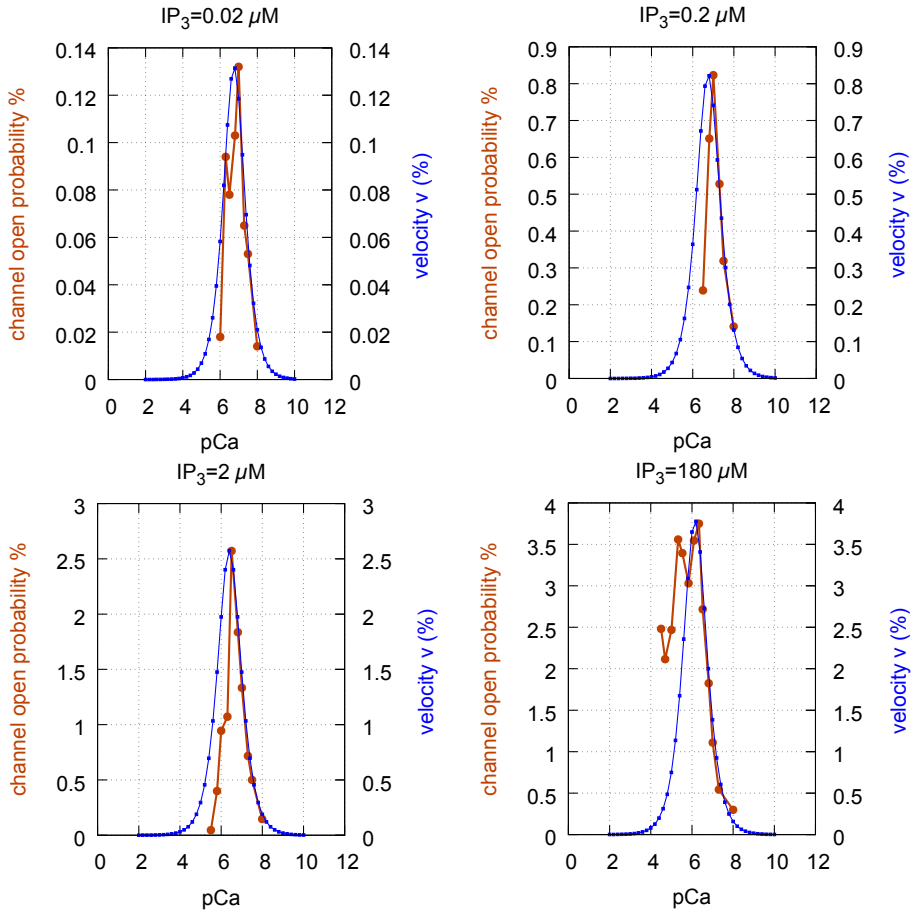

Figure S2. Experimental channel open probability in comparison with fitted v as a function of IP_3 and cytosolic calcium concentrations. Experimental results shown as dark-orange dots (left ordinate) are redrawn from Kaftan et al. [2]. Fitted v values in % (channel open propability) are given in blue (right ordinate). Parameter values (from left to right and down): IP_3=0.02μM: $K_1^{IP3R\cdot Ca_{ER}} = K_1^{IP3R} = K_2^{IP3R\cdot Ca_{ER}} = K_2^{IP3R} = 1.78 \times 10^{-7}$M, $V_{max} = 0.4$ %; IP_3=0.2μM: $K_1^{IP3R\cdot Ca_{ER}} = K_1^{IP3R} = K_2^{IP3R\cdot Ca_{ER}} = K_2^{IP3R} = 1.78 \times 10^{-7}$M, $V_{max} = 2.5$ %; IP_3=2μM: $K_1^{IP3R\cdot Ca_{ER}} = K_1^{IP3R} = K_2^{IP3R\cdot Ca_{ER}} = K_2^{IP3R} = 3.98 \times 10^{-7}$M, $V_{max} = 7.8$ %; IP_3=180μM: $K_1^{IP3R\cdot Ca_{ER}} = K_1^{IP3R} = K_2^{IP3R\cdot Ca_{ER}} = K_2^{IP3R} = 7.08 \times 10^{-7}$M, $V_{max} = 11.5$ %. K_M=0.01 μM and Ca_{ER}=1 μM in all four fits. pCa $= -\log_{10}$[Ca].

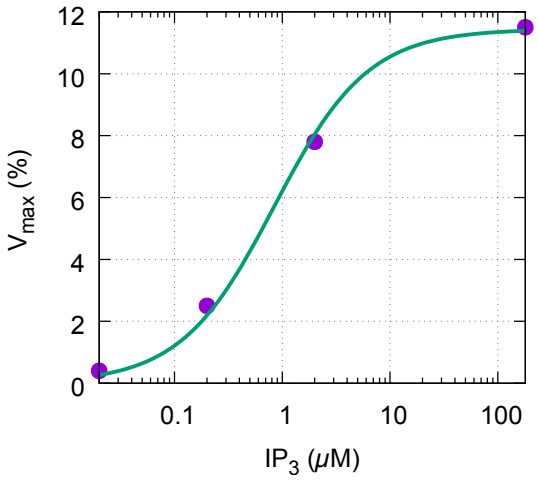

Figure S3. Obtained V_{max} values as a function of IP_3 concentration. Purple dots show V_{max} values while the green line shows the fitted function $f(x) = a{\cdot}x/(b+x)$. The values of a and b were determined to (11.44±0.30) % and 0.844±0.105 μM, respectively. To see the quality of the fit the abscissa has a logarithmic scale.

$$^{\mathrm{Ca_{cyt}}}\mathrm{IP_3R_{IP3}}^{*}\bullet \mathrm{Ca^{2+}_{ER}} + 2\,\mathrm{Ca^{2+}_{cyt}} \rightleftarrows {}^{\mathrm{Ca_{cyt_3}}}\,\mathrm{IP_3R_{IP3}}\bullet \mathrm{Ca^{2+}_{ER}} \tag{S17}$$

with

$$K_2^{IP3R{\cdot}Ca_{ER}} = \frac{(\mathrm{Ca^{2+}_{cyt}})^2(^{\mathrm{Ca_{cyt}}}\mathrm{IP_3R_{IP3}}^{*}\bullet \mathrm{Ca^{2+}_{ER}})}{(^{\mathrm{Ca_{cyt_3}}}\mathrm{IP_3R_{IP3}}\bullet \mathrm{Ca^{2+}_{ER}})} \tag{S18}$$

While the Ca transport rate v out of the ER is still given by Eq. S14

$$v = \frac{V_{max}\cdot(\mathrm{Ca^{2+}_{ER}})}{f_{IP3R}\cdot K_M + f_{IP3R{\cdot}Ca_{ER}}\cdot(\mathrm{Ca^{2+}_{ER}})} \tag{S19}$$

the f-functions are changed to

$$f_{IP3R} = 1 + \frac{K_2^{IP3R}}{\mathrm{Ca^{2+}_{cyt}}} + \frac{(\mathrm{Ca^{2+}_{cyt}})^2}{K_1^{IP3R}} \tag{S20}$$

and

$$f_{IP3R{\cdot}Ca_{ER}} = 1 + \frac{K_2^{IP3R{\cdot}Ca_{ER}}}{\mathrm{Ca^{2+}_{cyt}}} + \frac{(\mathrm{Ca^{2+}_{cyt}})^2}{K_1^{IP3R{\cdot}Ca_{ER}}} \tag{S21}$$

Using Eq. S14 with the new f-functions provide better overall results (Fig. S4), but requires that the activating dissociation constants K_1^{IP3R}, $K_1^{IP3R{\cdot}Ca_{ER}}$ are different from K_2^{IP3R} and $K_2^{IP3R{\cdot}Ca_{ER}}$. The very low values of K_1^{IP3R} and $K_1^{IP3R{\cdot}Ca_{ER}}$ (Fig. S4) indicate that the second-order cooperative and inhibitory binding by cytosolic Ca is strong.

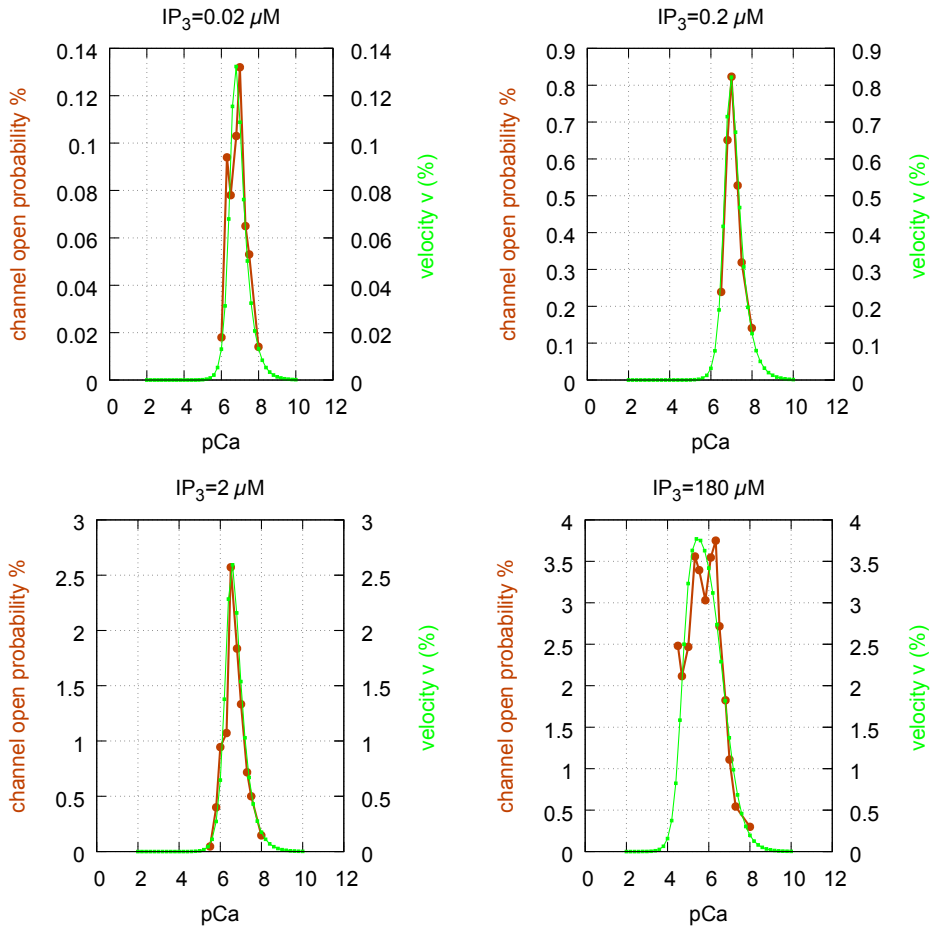

Figure S4. Fit of dicalcic v as a function of IP_3 and cytosolic calcium concentrations with a second-order cooperative binding for the Ca inhibiting step. Experimental results shown as dark-orange dots (left ordinate) as in Fig. S2 while v values are given in green (right ordinate). Parameter values (drom left to right and down): IP_3=0.02μM: $K_1^{IP3R\cdot Ca_{ER}} = K_1^{IP3R} = 1.26 \times 10^{-14}$M, $K_2^{IP3R\cdot Ca_{ER}} = K_2^{IP3R} = 7.94 \times 10^{-7}$M, $V_{max} = 1.07$ %; IP_3=0.2μM: $K_1^{IP3R\cdot Ca_{ER}} = K_1^{IP3R} = 3.98 \times 10^{-15}$M, $K_2^{IP3R\cdot Ca_{ER}} = K_2^{IP3R} = 6.31 \times 10^{-7}$M, $V_{max} = 8.15$ %; IP_3=2μM: $K_1^{IP3R\cdot Ca_{ER}} = K_1^{IP3R} = 5.01 \times 10^{-14}$M, $K_2^{IP3R\cdot Ca_{ER}} = K_2^{IP3R} = 7.94 \times 10^{-7}$M, $V_{max} = 14.2$ %; IP_3=180μM: $K_1^{IP3R\cdot Ca} = K_1^{IP3R} = 3.98 \times 10^{-10}$M, $K_2^{IP3R\cdot Ca} = K_2^{IP3R} = 2.0 \times 10^{-7}$M, $V_{max} = 4.15$ %. K_M=0.01 μM and Ca_{ER}=1 μM in all four fits. pCa = $-\log_{10}[Ca]$.

Fig. S5 shows that for the cooperative case V_{max} increases logarithmically with increasing IP_3 concentration but becomes low again at IP_3=180μM (see legend of Fig. S4).

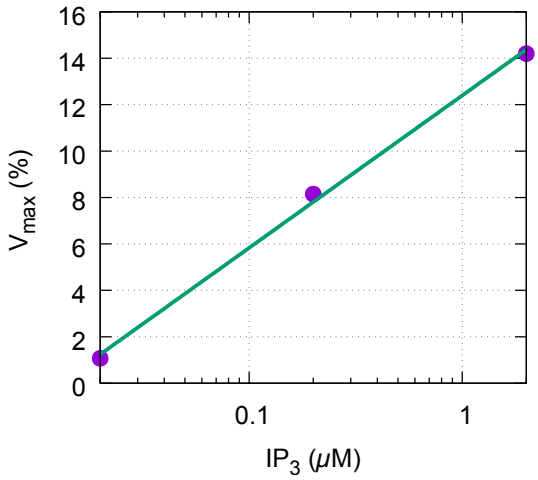

Figure S5. Obtained V_{max} values as a function of IP_3 concentration in the cooperative model. Purple dots show V_{max} values while the green line shows the fitted function $f(x) = a + b \cdot \log_{10}(x)$. The values of a and b were determined to (12.40±0.32)% and (6.57±0.30) %/($\log_{10}(\mu$M)), respectively. The V_{max} value for IP_3=180μM is not included in this plot.

How the fits were performed

The data were extracted from Figure 2 from Kaftan et al. [2] using GraphClick (https://graphclick.en.softonic.com/mac). For each IP_3 concentration the cytosolic calcium concentrations were recalculated to pCa values and imported into Excel, which also contained v either from Eq S14 or from Eq S19 as a function of pCa.

The dissociation constants K_1^{IP3R} (K1E), $K_1^{IP3R \cdot Ca_{ER}}$ (K1ES), K_2^{IP3R} (K2E), $K_2^{IP3R \cdot Ca_{ER}}$ (K2ES), and V_{max} (Vmax) were used as adjustable parameters (Excel variable names in parentheses). An eye-balled fit of v to the experimental data was performed by manually changing the parameters K1E, K1ES, K2E, K2ES, and Vmax within each Excel file. The Excel files are found in the folders `'dicalcic model (no cooperativity)'` and `'dicalcic model (cooperative inhibition)'`.

References

1. Tipton KF, Dixon HB. Effects of pH on Enzymes. Methods in Enzymology. 1979;63:183–234.
2. Kaftan EJ, Ehrlich BE, Watras J. Inositol 1, 4, 5-trisphosphate ($InsP_3$) and calcium interact to increase the dynamic range of $InsP_3$ receptor-dependent calcium signaling. The Journal of General Physiology. 1997;110(5):529–538.